

Journal of Basics and Applied Sciences Research (JOBASR) ISSN (print): 3026-9091, ISSN (online): 1597-9962

Volume 1(1) IPSCFUDMA 2025 Special Issue DOI: https://dx.doi.org/10.4314/jobasr.v1i1.2s



Synthesis and Characterization of Amorphous Silica Nanoparticles from Oil Palm Leaf Biomass via Acid and Thermal Treatments



Adikwu Gowon Jacob^{1*}, Abdulkarim Shehu Salihu¹, Ojochide Monday Ameh¹, Aminu Garba Abdullahi², Yusuf Mamman² & Abdulazeez Lawal Maigoro¹

- ¹Department of Industrial Chemistry, Faculty of Physical Sciences, Federal University Dutsin-Ma, P.M.B. 5001 Dutsin-Ma, Katsina State, Nigeria
- ²Department of Chemistry, Faculty of Physical Sciences, Federal University Dutsin-Ma, P.M.B. 5001 Dutsin-Ma, Katsina State, Nigeria
- *Corresponding Author Email: gjacob@fudutsinma.edu.ng

ABSTRACT

This study describes a method of transforming underutilized oil palm leaf biomass into silica. In the present study, a simple method of preparing amorphous silicais reported. The preparation consists of two steps: (1) acidtreatment of oil palm leaf biomass with concentrated HCl, and (2) calcination of the acid-treatedoil palm leaf biomass at 600 °C. The oil palm leaf biomass, acidtreated oil palm leaf biomass and the resulting silica were characterized by Fourier-transform infrared spectroscopy (FTIR), X-ray diffraction (XRD), and scanning electron microscopy (SEM). The results from the synthesis showed that a silica yield of 28.9% was obtained. FTIRspectroscopy revealed five absorption peaks at 567, 800, 955, 1055, 1633 and 3392 cm⁻¹ in the spectrum of the heat-treated oil palm leaf biomass which indicates the formation of silica. Also, the peaks at 1445, 2847, 2920 cm⁻¹ attributed to C-H bonds of -CH₂ or -CH₃ groups in the raw oil palm leaf biomass disappeared after the acid- and thermal-treatments. X-ray diffractogram of the oil palm leaf biomass showed multiple 2θ peaks from 20-55°, typical of crystalline structure, which disappeared and formed a single broad or halo peak centered at $2\theta = 22.1^{\circ}$ afterthe treatments, with crystallinity index of 9.43%, confirming the formation of an amorphous silica phase. SEM microgram of the thermal-treated oil palm leaf biomass showed agglomerated particleswith spherical morphology and particlesize ranging from 75-90 nm, supporting the formation of silica nanoparticles. Notably, this study revealed that amorphous silica could be prepared using a simple, energy-efficient method.

Keywords:

Oil palm leaf, FTIR spectroscopy, X-ray diffraction, Morphology, Amorphous silica

INTRODUCTION

The global demand for sustainable materials and the pressing need to address agricultural waste in the environment have intensified research efforts toward valorizing biomass wastes into high-value products. The oil palm industry generates substantial quantities of lignocellulosic waste (Wu et al., 2017), including empty fruit bunches, palm kernel shells, palm oil mill effluent, and oil palm leaves, which are often underutilized or disposed of through environmentally problematic methods such as open burning (Sulaiman et al., 2011). Oil palm leaves, in particular, constitute a significant portion of this waste stream, with each mature palm tree producing approximately 10-15 fronds annually. equivalent to 15-20 kg of dry biomass per tree (Febriani et al., 2020). Traditional disposal methods for oil palm leaves include mulching and burning, both of which fail

to capture the inherent value of these materials. Recent studies have revealed that oil palm biomass contains substantial amounts of silica, typically ranging from 2-8% by weight, making it an attractive precursor for silica production (Osman & Sapawe, 2020). This discovery has opened new avenues for converting agricultural waste into valuable silica-based materials with diverse industrial applications.

Traditional silica production depends heavily on energy-intensive processes involving high-purity quartz sand and sodium carbonate at temperatures exceeding 1400°C, resulting in significant carbon emissions and environmental concerns (Taiye *et al.*, 2024). Moreover, the depletion of high-quality silica sand reserves has prompted researchers to explore alternative, sustainable sources for silica production. The development of efficient methods for producing

high-quality amorphous silica from oil palm leaf biomass holds significant potential for addressing both waste management challenges and the growing demand for sustainable silica sources. Previous studies have demonstrated the feasibility of extracting silica from various parts of oil palm biomass, but comprehensive studies focusing specifically on oil palm leaves remain limited (Nelson *et al.*, 2023; Bukit *et al.*, 2022). The present study addresses this knowledge gap by developing a simple and efficient method for producing amorphous silica from oil palm leaf biomass.

MATERIALS AND METHODS

Materials

Fresh oil palm leaves were collected from a mature oil palm plantation in Ikpochi Owukpa, Benue State, following a reported sampling protocol or biomass characterization studies (Aliyu *et al.*, 2025). Concentrated hydrochloric acid (HCl, 37% purity) was obtained from Merck KGaA (Darmstadt, Germany). All chemicals used were of analytical grade and used without further purification. Distilled water was used throughout the experiment to minimize contamination from metallic impurities (Etong *et al.*, 2014).

Sample Preparation

The collected oil palm leaves were initially cleaned to remove dirt, dust, and other foreign materials, then washed thoroughly with distilled water and air-dried at ambient temperature (30 °C) for 48 h. The dried leaves were subsequently oven-dried at 105°C for 24 h to achieve constant weight and eliminate residual moisture content (Rovani *et al.*, 2019). The dried biomass was mechanically ground using a laboratory mill (Retsch SM 100, Germany), and sieved through a 250-mesh screen to obtain a uniform particle size distribution ranging from 60-75 µmto optimize surface area for subsequent chemical treatments (Simanjuntak *et al.*, 2021).

Acid Pretreatment

The acid pretreatment process was conducted following the modified procedure described by Rahman *et al.* (2015). Approximately 50.0 g of the ground oil palm leaf biomass was mixed with 500 mL of concentrated HCl (37%) in a 1000 mL round-bottom flask equipped with a

reflux condenser. The mixture was heated at 80 °C for 4 h under continuous magnetic stirring at 300 rpm to ensure uniform acid penetration and effective removal of metallic impurities, including potassium, calcium, magnesium, and iron (Jacob $et\ al.$, 2022a). The acid-to-biomass ratio of 10:1 (v/w) was selected based on preliminary optimization studies that demonstrated maximum impurity removal while minimizing cellulose degradation.

The mixture was cooled to room temperature and filtered using Whatman No. 1 filter paper. The acid-treated biomass was extensively washed with distilled water until the filtrate reached neutral pH (7.0), as confirmed using a calibrated pH meter (Hanna Instruments HI-2020, Romania). The washed biomass was then dried in an oven at 105°C for 12 h to remove residual moisture and prepare it for thermal treatment (Prempeh *et al.*, 2021).

Thermal Treatment

The thermal treatment was performed by a programmable muffle furnace (Nabertherm LHT 02/17, Germany) following a reported method in literature (Janowska-Renkas *et al.*, 2025). The acid-treated oil palm leaf biomass (20.0 g) was placed in alumina crucibles and heated at an initial rate of 10 °C/min to 600°C, and maintained at 600°C for 3 h under atmospheric condition. This temperature allowed complete decomposition of organic matter but prevented silica crystallization (Jacob *et al.*, 2022a).

The furnace was allowed to cool naturally to room temperature over 12 h to prevent thermal shock and potential structural changes in the silica product. The resulting white powder was carefully collected, weighed to determine yield, and stored in sealed glass containers under desiccated conditions to prevent moisture absorption prior to characterization (Johnson *et al.*, 2024). Fig. 1 graphically summarizes the various steps involved inpreparing the silica. The percentage yield of the silica was calculated using the Equation 1. Persentage Yield

$$= \frac{\text{Weight of silica obtained}}{\text{Weight of thermal} - \text{treated biomass}} x100 \quad (1)$$

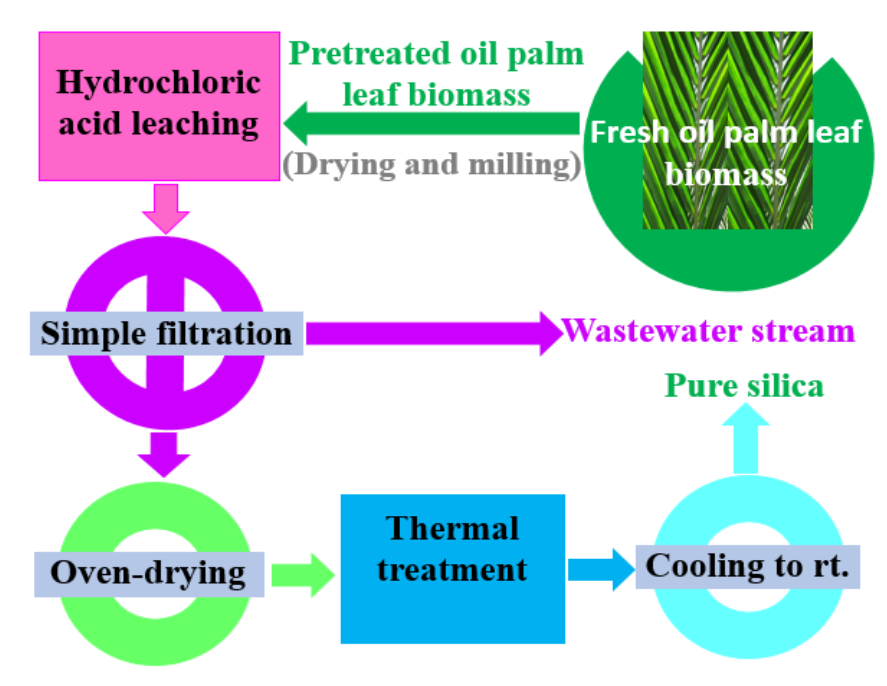


Fig. 1: Schematic flow diagram for armopous silica preparation from leaf of oil palm biomass

Characterization Techniques

Fourier Transform Infrared (FTIR) Spectroscopy

FTIR analysis was conducted using a Perkin Elmer Spectrum 100 FTIR spectrometer equipped with an attenuated total reflectance (ATR) accessory. Spectra were recorded in the wavenumber range of 4000-400 cm⁻¹ with a resolution of 4 cm⁻¹ and 32 scans per sample to ensure an adequate signal-to-noise ratio. Approximately 2.0 mg of sample with 200 mg of spectroscopic grade KBrwere mixed and pressed into transparent pellets using a hydraulic press at 10 tons pressure for 2 min (Prabha *et al.*, 2021).

X-ray Diffraction (XRD) Analysis

XRD diffractograms were collected using a Rigaku Mini Flex 600 X-ray diffractometer equipped with Cu K α radiation (λ = 1.5406 Å) operating at 40 kV and 15 mA. The three samples were scanned over a 2 θ range of 10-80° with a step size of 0.02° and a scanning rate of 2°/min to ensure adequate peak resolution (Chryssou & Lampi. 2024). For each, 1.0 g of the sample was mounted on a zero-background silicon holder and leveled for uniform surface coverage. Phase identification was performed using the International Centre for Diffraction Data (ICDD) database, and the degree of crystallinity was calculated using the method described by Montoya-Escobar *et al.* (2022).

Scanning Electron Microscopy (SEM) Analysis

Surface morphology and particle size analysis were conducted using a JEOL JSM-6701F field emission scanning electron microscope operating at accelerating

voltages of 5-15 kV. Samples were prepared by mounting on aluminum stubs using double-sided carbon tape and sputter-coated with a thin layer of gold (10 nm thickness) using a JEOL JFC-1600 auto fine coater to enhance conductivity and prevent charging effects (Fukushina *et al.*, 2024). Images were captured at various magnifications ranging from 1,000× to 100,000× to observe both overall morphology and detailed surface features. Particle size distribution was determined by measuring at least 200 individual particles using ImageJ software (version 1.53k) (Al-Khafaji *et al.*, 2020).

RESULTS AND DISCUSSION

The FTIR spectra of the oil palm leaf biomass, acid-treated and heat-treated samples are shown in Fig.2. Generally, multiple peaks were found from 554-3392 cm⁻¹ in the spectra. The FTIR spectrum of the untreated oil palm leaf biomass (Fig. 2a) exhibits characteristic peaks that reflect the complex organic structure typical of lignocellulosic materials. A broad peak around 3315 cm⁻¹ corresponds to O–H stretching vibrations, which are associated with hydroxyl groups found in cellulose, hemicellulose, and lignin. The peak at 2920 cm⁻¹ is linked to C–H stretching from aliphatic compounds in the biomass.

A notable absorption at 1628 cm⁻¹ suggests the presence of carbonyl (C=O) groups, which likely originated from lignin and hemicellulose, whereas the peak at 1445 cm⁻¹ corresponds to C–H bending vibrations. Meanwhile, the peak at 1055 cm⁻¹ corresponds to C–O stretching found in both cellulose and hemicellulose, although Si–O stretching vibrations

may also contribute here but are largely hidden by the dominant organic signals. Additional peaks around 955 cm⁻¹ suggest C–O–C glycosidic linkages, and the peak at 800 cm⁻¹ indicates aromatic C–H out-of-plane bending, possibly with some input from Si–O–Si bending vibrations that remain covered by the organic components (Ramasamy *et al.*, 2023).

After the acid treatment (Fig. 2b), some noticeable changes in the spectrum indicate that much of the cellulose and hemicellulose has been removed, whereas silica becomes more enriched. The broad O–H stretching peak at 3315 cm⁻¹ has considerably reduced,

signifyingbreakdown and removal of hydroxyl-rich polysaccharides. Similarly, the decreased intensity of the carbonyl peak at 1628 cm⁻¹ supports the fact that the hemicellulose component has degraded under acidic conditions. The peak at 1055 cm⁻¹ becomes more distinct and intense, as the reduction in organic components uncovers the hidden Si–O stretching vibrations. The peak at 800 cm⁻¹ which is attributed to Si–O–Si bending vibrations, becomes more prominent, suggesting removal of the overlapping organic components (Mohd-Basri *et al.* 2021).

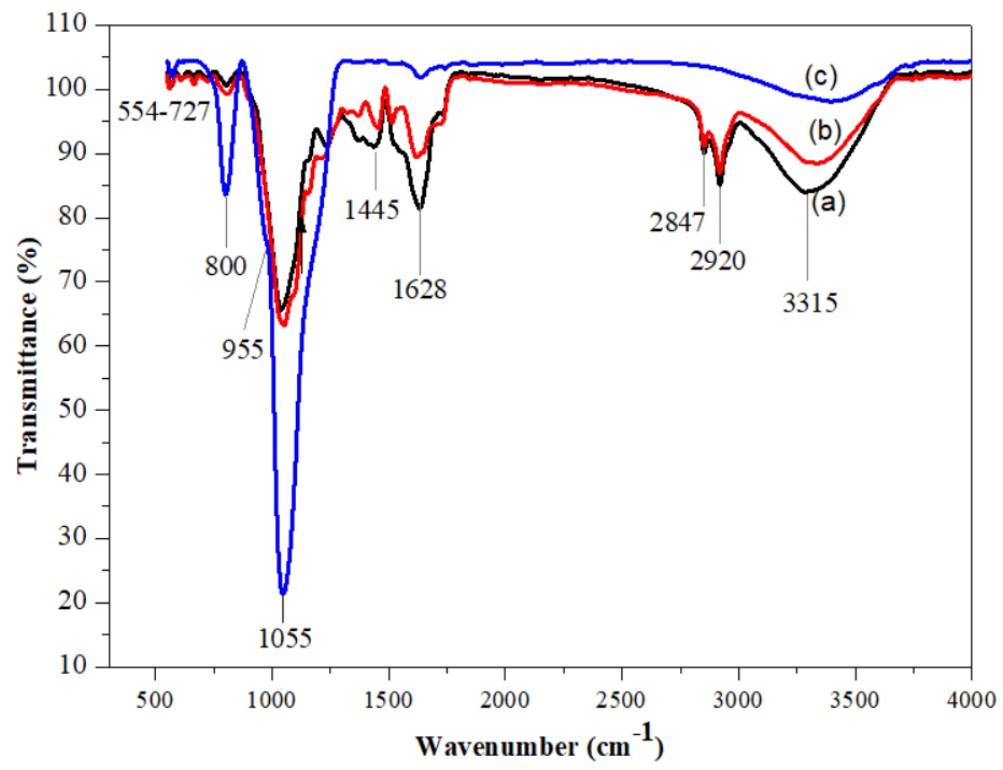


Fig. 2: FTIR spectra of (a) raw oil palm leaf biomass, (b) acid-treated oil palm leaf biomass and (c) thermal-treated acid-treated oil palm leaf biomass

With heat treatment, the spectrum (Fig. 2c) displays even more pronounced changes, highlighting substantial decomposition of the organic matrix and formation of well-structured silica. The O–H stretching peak at 3315 cm⁻¹ reaches its lowest intensity, reflecting the breakdown of remaining hydroxyl-containing compounds. Thermal treatment seems to promote condensation reactions that help form more organized silica networks. The Si–O stretching band at 1055 cm⁻¹ becomes sharp and intense, suggesting highly developed silica with minimal interference from organic residues. Likewise, the peak at 800 cm⁻¹ becomes most distinct among the three samples, demonstrating strong Si–O–Si bending vibrations consistent with condensed silica. Moreover, the multiplepeaks in the fingerprint region (554-727 cm⁻¹) are

well-resolved, suggestingthe presence of various Si–O deformation modes often seen in biomass-derived silica. Both treatments effectively convert the lignocellulosic material into silica by gradually removing the organic content while enriching the silica network. The gradual disappearance of organic peaks (C-H, C=O) and the emergence of inorganic silica peaks (Si-O-Si) suggested of pure silica was formed. The FTIR peaks observed in this study corroborate the previous study for silica extracted from rice husk (Mohd-Basri *et al.* 2021).

XRD pattern of the raw oil palm leaf biomass (Fig. 3a) exhibits some diffraction peaks that are typical to lignocellulosic materials. The multiple sharp and intense peaks at $2\theta = 23.1, 23.5, 24.3, 26.2, 27.1, 28.2, 29.4, 31.3, 32.2, 33.1. 36.1, 37.8, 38.4, 40.5, 45.7, 48.3,$

and 50.1°, shows the presence of various crystalline phases. These peaks correspond to the cellulose, hemicellulose, and lignin, and inorganic impurities.

After the acid treatment, the XRD pattern (Fig.3b) reveals a broad hump centered at $2\theta = 21.7^{\circ}$, with reduced peak sharpness that is characteristic of a partially amorphous silica phase, showing some short-range order (Jacob *et al.*, 2022b). The presence of this peak with reduced crystallinity is indicative of the degradation of cellulose, hemicellulose and lignin; and increased mineral phases, i.e., silica.

The thermal-treated sample (Fig.3c) displays a very broad and diffuse halo peak centered at $2\theta=22.1^\circ$, with the absence of sharp peaks, indicating a fully amorphous silica structure commonly obtained after calcination or chemical treatment of the biomass ash. The observed halo peak at $2\theta=22.1^\circ$ is a characteristic of the short-range atomic order in amorphous silica, further validating the successful synthesis of the amorphous silica (Rovani *et al.*, 2018), and supporting the results of the FTIR spectroscopy.

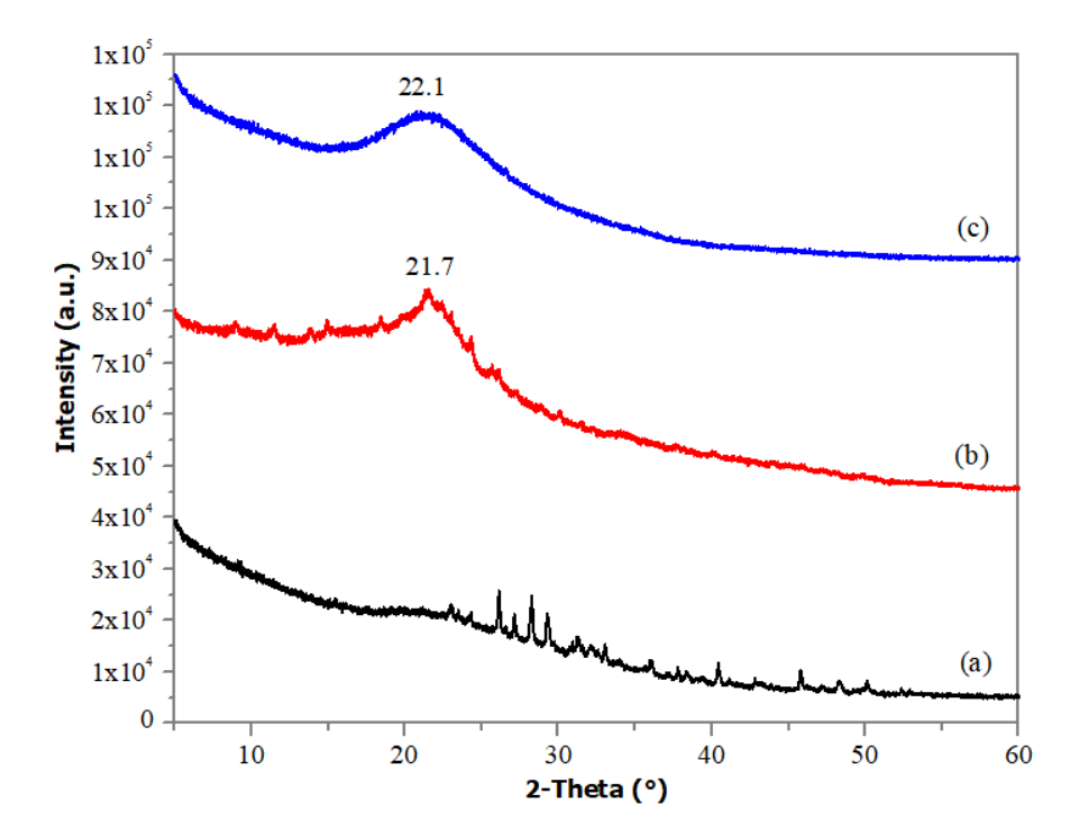


Fig. 3: XRD patterns of (a) raw oil palm leaf biomass, (b) acid-treated oil palm leaf biomass and (c) thermal-treated acid-treated oil palm leaf biomass

The crystallinity indices of the raw oil palm leaf biomass, acid-treated sample and thermal-treated sample were found to be 40.68%, 9.76% and 9.43% respectively. As shown, there is a clear progressive decrease in crystallinity from crystalline to semi-amorphous to amorphous structure (Fig. 3a-c). This progression is desirable for enhancing the performance of silica in adsorption, catalysis, and surface reactions. The results of the XRD study are consistent with the findings from silica obtained the rice husk and palm fruit bunch (Aliyu *et al.*, 2025).

The SEM image of (Fig.4) reveals that the silica particles prepared from oil palm leaf biomass show a nearly spherical and agglomerated morphology. The agglomeration of particles observed arises from the high surface energy and high hydrogen bonding between the abundant silanol groups (Si-OH) at the surface of the amorphous silica. The particles appear densely packed, forming clusters without sharp edges, indicative of typical amorphous silica. This morphology is consistent with biomass-derived silica sugarcane waste ash (Rovani *et al.*, 2018).

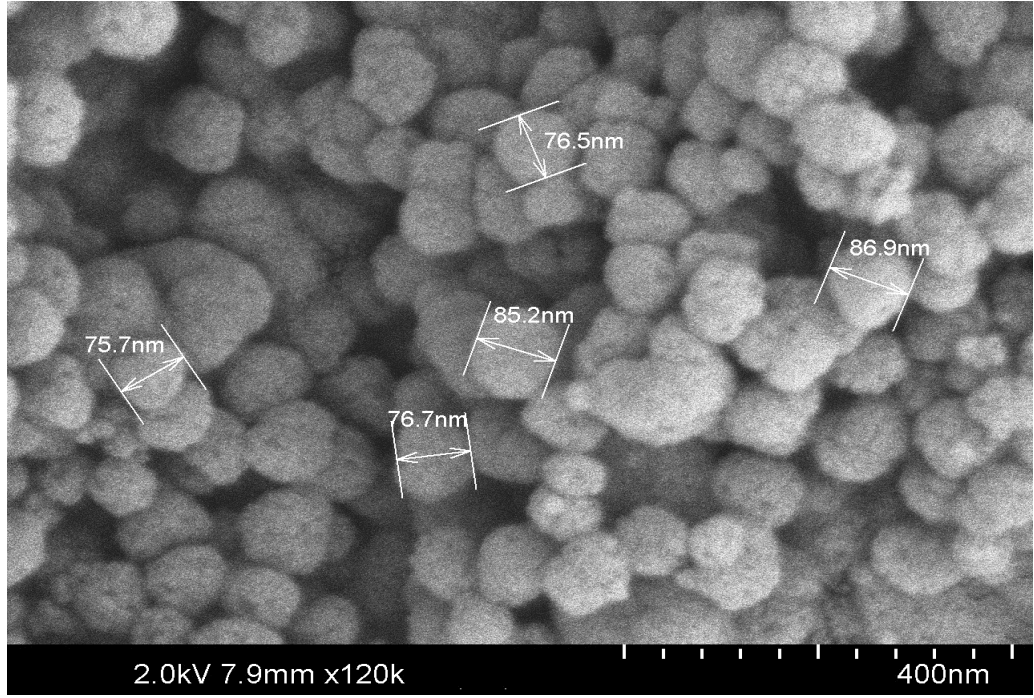


Fig. 4: SEM image of amorphous silica nanoparticles prepared from oil palm leaf biomass after acid and thermal treatments

The average particle size of the synthesized silica is within the range of 75-87 nm, as indicated by the annotated diameters. These values reflect nanoparticles domain of the ordered material of an amorphous silica structure. The nanosized silica has significant high surface area making it a promising material for applications in catalysis, adsorption, or nanocomposites (Al-Khafaji *et al.*, 2020).

In summary, the FTIR spectra showed that after the acid and thermal treatments, the peaks for the organic components (C-H, C-O, C=O) gradually disappeared whereas the characteristic siloxane group (Si-O-Si) strongly emerged. The XRD confirmed that an amorphous silica with low crystallinity of 9.43% was formed. The SEM revealed spherical shape silica nanoparticles with average diameter of $\sim 80.2~\rm nm,$ with high agglomeration from surface energy and hydrogen bonding of the silanol group that are readily available on the surface of the amorphous silica. Therefore, collective findings from FTIR, XRD, and SEM confirmed the successful conversion of crystalline oil palm leaf biomass into high-purity, amorphous silica nanoparticles.

CONCLUSION

The characterization with FTIR spectroscopy, XRD analysis, and SEM imaging provided a detailed understandings of the chemical structure, physical properties, and morphology of the synthesized silica. The loss of organic functional groups, the appearance of a broad XRD halo, and the observed nanosized morphology

collectively confirmed the successful synthesis of silica. Thus, the studyhas proved the formation of amorphous silica nanoparticles via an environmentallyfriendly and energy-efficient method utilizing the abundant renewable agricultural waste (i.e., oil palm leaf biomass) as a sustainable raw material. Since silica nanoparticles especially those from biogenic sources have high surface area andare exceptionally biocompatible with most biological systems, the silica obtained in this study can therefore be used fordrug delivery systems. Additionally, the silica can also be used in other applications such as adsorption and catalysis where high surface area-to-volume ratio is required. The findings contributed to the growing body of knowledge on biomass valorization and offered a sustainable approach for converting agricultural waste into valuable silica at relatively low temperature. Future works will focus on the use of other characterization techniques to understand the thermal stability and surface properties of silica nanoparticle from oil palm leaf biomass via the method used in this study.

REFERENCES

Al-Khafaji, M. A., Gaál, A., Wacha, A., Bóta, A., & Varga, Z. (2020). Particle size distribution of bimodal silica nanoparticles: A comparison of different measurement techniques. *Materials*, *13*(14), 3101.

Aliyu, A. S., Aliyu, U. S. A., Hamza, A. M., Nyakuma, B. B., Liman, M. S., Gaya, U. I., &Liman, M. M.

(2025). Synthesis and characterisation of rice husk and palm fruit bunch silica: compositional, structural, and thermal analyses. *Biomass Conversion and Biorefinery*, 15(3), 3533-3544.

Azat, S., Korobeinyk, A. V., Moustakas, K., & Inglezakis, V. J. (2019). Sustainable production of pure silica from rice husk waste in Kazakhstan. *Journal of cleaner production*, 217, 352-359.

Bukit, B. F., Frida, E., Humaidi, S., Sinuhaji, P., & Bukit, N. (2022). Optimization of palm oil boiler ash biomass waste as a source of silica with various preparation methods. *Journal of Ecological Engineering*, 23(8).

Chryssou, K., & Lampi, E. (2023). The X-ray diffraction pattern of the ash content on ignition at 900 C of a copy paper sample and its mechanical and optical properties. *Ann. Chem. Sci. Res*, *3*, 1-9.

Etong, D. I., Mustapha, A. O., Lawrence, I. G., Jacob, A. G., &Oladimeji, M. O. (2014). Nutritional and physicochemical properties of wheat (Triticumvulgare), cassava (Manihotesculenta) and sweet Potato (Ipomoea batatas) flours. *Pakistan Journal of Nutrition*, *13*(8), 439.

Febriani, A., Syafriana, V., Afriyando, H., & Djuhariah, Y. S. (2020). The utilization of oil palm leaves (Elaeisguineensis Jacq.) waste as an antibacterial solid bar soap. In *IOP conference series: Earth and environmental science* (Vol. 572, No. 1, p. 012038). IOP Publishing.

Fukushina, E., Sakamoto, T., & Takebe, H. (2023). Microstructural investigation of hydroxyapatite formation in bioactive borosilicate glass. *Journal of the Ceramic Society of Japan*, *131*(10), 843-849.

Jacob, A. G., Teo, H. L., Mahat, N. A., &Wahab, R. A. (2022a). Oil palm leaves-based silica/magnetite/graphene oxide composite as carrier. In Rahman, R.A., &Shaarani, S.Md (1st Ed.). Enzyme *Immobilization for Bioprecessing* (pp.193-234). Penerbit Press, UTM, Malaysia.

Jacob, A. G., Wahab, R. A., Chandren, S., Jumbri, K., &Mahmood, W. M. A. W. (2022b). Physicochemical properties and operational stability of Taguchi design-optimized Candida rugosa lipase supported on biogenic silica/magnetite/graphene oxide for ethyl valerate synthesis. *Advanced Powder Technology*, *33*(1), 103374.

Janowska-Renkas, E., Król, A., Klementowski, I., &Sokolski, M. (2025). Hemp Concrete with Mineral Additives as a Durable and Fire-Resistant Material in Green Construction. *Materials*, *18*(9), 1905.

Johnson, R. T., Kim, S. H., & Patel, V. K. (2023). FTIR

spectroscopic analysis of biomass-derived silica: Identification of key functional groups. *Spectrochimica Acta Part A: Molecular and Biomolecular Spectroscopy*, 289, 122245.

MohdBasri, M. S., Mustapha, F., Mazlan, N., & Ishak, M. R. (2021). Rice husk ash-based geopolymer binder: Compressive strength, optimize composition, FTIR spectroscopy, microstructural, and potential as fire-retardant material. *Polymers*, *13*(24), 4373.

Montoya-Escobar, N., Ospina-Acero, D., Velásquez-Cock, J. A., Gómez-Hoyos, C., Serpa Guerra, A., GañanRojo, P. F., ... & Stefani, P. M. (2022). Use of fourier series in X-ray diffraction (XRD) analysis and fourier-transform infrared spectroscopy (FTIR) for estimation of crystallinity in cellulose from different sources. *Polymers*, *14*(23), 5199.

Nelson, E. S., Iyuke, S., Daramola, M. O., &Okewale, A. (2023). Extraction and characterization of silica from empty palm fruit bunch (EPFB) Ash. Processes, 11(6), 1684.

Osman, N. S., &Sapawe, N. (2020). High purity and amorphous silica (SiO₂) prepared from oil palm frond (OPF) through sol–gel method. *Materials Today: Proceedings*, *31*, 228-231.

Prabha, S., Durgalakshmi, D., Rajendran, S., & Lichtfouse, E. (2021). Plant-derived silica nanoparticles and composites for biosensors, bioimaging, drug delivery and supercapacitors: a review. *Environmental chemistry letters*, 19(2), 1667-1691.

Prempeh, C. O., Formann, S., Schliermann, T., Dizaji, H. B., &Nelles, M. (2021). Extraction and characterization of biogenic silica obtained from selected agro-waste in Africa. *Applied Sciences*, 11(21), 10363.

Ramasamy, S. P., Veeraswamy, D., Ettiyagounder, P., Arunachalam, L., Devaraj, S. S., Krishna, K., & Sakrabani, R. (2023). New insights into method development and characterization of amorphous silica from wheat straw. *Silicon*, *15*(12), 5049-5063.

Rahman, N. A., Widhiana, I., Juliastuti, S. R., & Setyawan, H. (2015). Synthesis of mesoporous silica with controlled pore structure from bagasse ash as a silica source. *Colloids and Surfaces A: Physicochemical and Engineering Aspects*, 476, 1-7.

Rovani, S., Santos, J. J., Corio, P., & Fungaro, D. A. (2018). Highly pure silica nanoparticles with high

adsorption capacity obtained from sugarcane waste ash. ACS omega, 3(3), 2618-2627.

Rovani, S., Santos, J. J., Corio, P., & Fungaro, D. A. (2019). An alternative and simple method for the preparation of bare silica nanoparticles using sugarcane waste ash, an abundant and despised residue in the Brazilian industry. *Journal of the Brazilian Chemical Society*, *30*, 1524-1533.

Simanjuntak, W., Pandiangan, K. D., Sembiring, Z., Simanjuntak, A., & Hadi, S. (2021). The effect of crystallization time on structure, microstructure, and catalytic activity of zeolite-A synthesized from rice husk silica and food-grade aluminum foil. *Biomass and Bioenergy*, 148, 106050.

Sulaiman, F., Abdullah, N., Gerhauser, H., & Shariff, A. (2011). An outlook of Malaysian energy, oil palm industry and its utilization of wastes as useful resources. *Biomass and bioenergy*, 35(9), 3775-3786.

Taiye, M. A., Hafida, W., Kong, F., & Zhou, C. (2024). A review of the use of rice husk silica as a sustainable alternative to traditional silica sources in various applications. *Environmental Progress & Sustainable Energy*, 43(6), e14451.

Wu, Q., Qiang, T. C., Zeng, G., Zhang, H., Huang, Y., & Wang, Y. (2017). Sustainable and renewable energy from biomass wastes in palm oil industry: A case study in Malaysia. *International Journal of Hydrogen Energy*, 42(37), 23871-23877